

# Fractional-Order Hybrid Control of Robot Manipulators

J. A. Tenreiro Machado and Abilio Azenha

Department of Electrical and Computer Engineering, Faculty of Engineering, University of Porto  
Rua dos Bragas, 4099 Porto Codex, Portugal

Phone: 351-2-317105, Fax: 351-2-2003610, E-mail: jtm@fe.up.pt, azenha@tom.fe.up.pt

## ABSTRACT

In this paper it is studied the implementation of fractional-order algorithms in the position/force hybrid control of robotic manipulators. The system robustness and performances are analysed, in terms of time responses, and compared with other control approaches. Moreover, it is also investigated the effect of nonlinear phenomena at the robot joints such as nonlinear friction, dynamic backlash and flexibility.

## 1. INTRODUCTION

In the early eighties Raibert and Craig [1] introduced the concept of force control based on the hybrid algorithm. Since then, several researchers [2] developed these ideas and proposed new algorithms such as the impedance controller. Problems with position/force control are further investigated in [3-4], while more recent studies of this algorithm can be found in [5-7].

This paper studies the position/force control of robot manipulators, required in processes that involve contact between the arm end-effector and the environment, using fractional-order algorithms. The application of the fractional derivatives and integrals (FDIs) is still in a research stage, but the recent progress in the areas of chaos and fractals reveals promising aspects for future developments [12-14].

In this line of thought, the article is organised as follows. Section two introduces the position/force hybrid control scheme. Section three formulates the FDI algorithms while section four presents several experiments for robots both with ideal and nonideal joints. Finally, section five outlines the main conclusions.

## 2. THE HYBRID CONTROLLER

The dynamic equation of an ideal (*i.e.* rigid-link, rigid-joint) robot with  $n$  links interacting with the environment is:

$$\tau = H(q)\ddot{q} + c(q, \dot{q}) + g(q) - J^T(q)F \quad (1)$$

Here  $\tau$  is the  $n \times 1$  vector of actuator torques,  $q$  is the  $n \times 1$  vector of joint coordinates,  $H(q)$  is the  $n \times n$  inertia matrix,  $c(q, \dot{q})$  is the  $n \times 1$  vector of centrifugal/Coriolis terms and  $g(q)$  is the  $n \times 1$  vector of gravitational effects. The  $n \times m$

matrix  $J^T(q)$  is the transpose of the Jacobian matrix of the robot and  $F$  is the  $m \times 1$  vector of the force that the ( $m$ -dimensional) environment exerts in the robot end-effector. In this study we shall adopt as prototype manipulator the 2R robot with dynamics given by:

$$H(q) = \begin{bmatrix} (m_1 + m_2)r_1^2 + m_2r_2^2 + & m_2r_2^2 + m_2r_1r_2C_2 \\ +2m_2r_1r_2C_2 + J_{1m} + J_{1g} & \\ m_2r_2^2 + m_2r_1r_2C_2 & m_2r_2^2 + J_{2m} + J_{2g} \end{bmatrix} \quad (2a)$$

$$c(q, \dot{q}) = \begin{bmatrix} -m_2r_1r_2S_2\dot{q}_2^2 - 2m_2r_1r_2S_2\dot{q}_1\dot{q}_2 \\ m_2r_1r_2S_2\dot{q}_1^2 \end{bmatrix} \quad (2b)$$

$$g(q) = \begin{bmatrix} g(m_1r_1C_1 + m_2r_1C_1 + m_2r_2C_{12}) \\ gm_2r_2C_{12} \end{bmatrix} \quad (2c)$$

$$J^T(q) = \begin{bmatrix} -r_1S_1 - r_2S_{12} & r_1C_1 + r_2C_{12} \\ -r_2S_{12} & r_2C_{12} \end{bmatrix} \quad (2d)$$

where  $C_i = \cos(q_i)$ ,  $C_{ij} = \cos(q_i + q_j)$ ,  $S_i = \sin(q_i)$ ,  $S_{ij} = \sin(q_i + q_j)$ . The numerical values adopted for the 2R robot are shown in Table I while the constraint plane is determined by the angle  $\theta$  as depicted in Fig. 1.

| $i$ | $m_i$<br>(Kg) | $r_i$<br>(m) | $J_{im}$<br>(Kgm <sup>2</sup> ) | $J_{ig}$<br>(Kgm <sup>2</sup> ) |
|-----|---------------|--------------|---------------------------------|---------------------------------|
| 1   | 0.5           | 1.0          | 1.0                             | 4.0                             |
| 2   | 6.25          | 0.8          | 1.0                             | 4.0                             |

Table I The 2R robot parameters.

The contact of the robot with the constraint surface is modelled through a linear system with a mass  $M$ , a damping  $B$  and a stiffness  $K$  with dynamics:

$$F = M\ddot{x} + B\dot{x} + Kx \quad (3)$$

The schematic structure of the position/force hybrid control algorithm is depicted in Fig. 2. The diagonal matrix  $S$  is the  $n \times n$  selection matrix with elements equal to one (zero) in the position (force) controlled directions and  $I$  is the  $n \times n$  identity

matrix. In this paper we consider the  $y_C(x_C)$  Cartesian coordinates to be position (force) controlled:

$$\mathbf{S} = \begin{bmatrix} 0 & 0 \\ 0 & 1 \end{bmatrix} \quad (4a)$$

$$\mathbf{J}_C(\mathbf{q}) = \begin{bmatrix} -r_1 C_{\theta_1} - r_2 C_{\theta_{12}} & -r_2 C_{\theta_{12}} \\ r_1 S_{\theta_1} + r_2 S_{\theta_{12}} & r_2 S_{\theta_{12}} \end{bmatrix} \quad (4b)$$

where  $C_{\theta_1} = \cos(\theta - q_1)$ ,  $C_{\theta_{12}} = \cos(\theta - q_1 - q_2)$ ,  $S_{\theta_1} = \sin(\theta - q_1)$  and  $S_{\theta_{12}} = \sin(\theta - q_1 - q_2)$ .

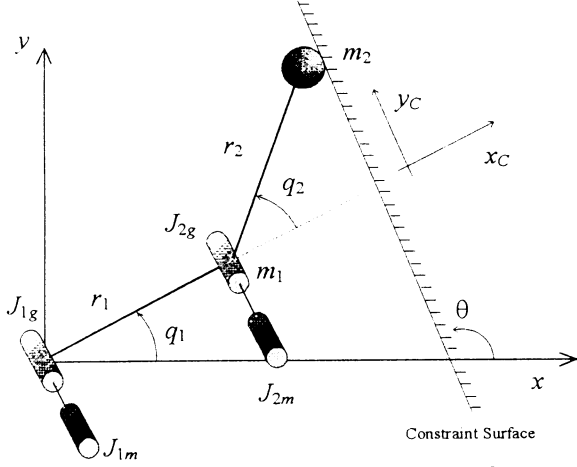


Figure 1 The 2R robot and the constraint surface.

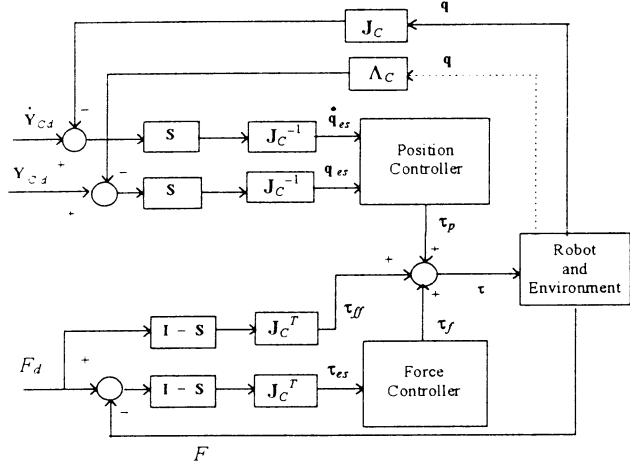


Figure 2 Block diagram of the position/force hybrid control scheme.

### 3. FRACTIONAL-ORDER ALGORITHMS

In this section we present the FDI controllers, adopted both at the position and force control loops.

The mathematical definition of a derivative or integral of fractional order has been the subject of several different approaches. For example, a “direct” definition based on the concept of fractional differential of order  $\alpha$ , is due to Letnikov (1868) and leads to the expression for  $D^\alpha$ , the fractional derivative of order  $\alpha$ :

$$D^\alpha x(t) = \lim_{h \rightarrow 0} \left[ \frac{1}{h^\alpha} \sum_{k=0}^{\infty} (-1)^k \binom{\alpha}{k} x(t - kh) \right] \quad (5a)$$

$$\binom{\alpha}{k} = \frac{\Gamma(\alpha + 1)}{\Gamma(k + 1)\Gamma(\alpha - k + 1)} \quad (5b)$$

where  $\Gamma$  is the gamma function and  $h$  is the time increment. Therefore, for a discrete-time control algorithm, with sampling period  $T$ , this formula can be approximated through a  $r$ -th order truncated series [14], resulting the following equation in the  $z$ -domain:

$$Z\{D^\alpha x(t)\} \approx \left\{ \frac{1}{T^\alpha} \sum_{k=0}^r (-1)^k \frac{\Gamma(\alpha + 1)z^{-k}}{k! \Gamma(\alpha - k + 1)} \right\} X(z) \quad (6)$$

Clearly, in order to have good approximations, we must have a large number of terms and a small sampling period. Table II shows the numerical values of the FDI controllers adopted in this study. These parameters were tuned by trial and error and represent a compromise between fast transients and large overshoots. The subscripts  $P$  or  $F$  stand for the position or force loops and the parameter  $K$  for a gain constant that is multiplied with the FDI truncated series.

| Joint $i$ | $K_{P_i}$ | $K_{F_i}$ | $\alpha_{P_i}$ | $\alpha_{F_i}$ | $r_{P_i}$ | $r_{F_i}$ |
|-----------|-----------|-----------|----------------|----------------|-----------|-----------|
| 1         | $10^5$    | $10^3$    | 1/2            | -1/5           | 17        | 17        |
| 2         | $10^5$    | $10^3$    | 1/2            | -1/5           | 17        | 17        |

Table II Numerical values of the FDI controllers.

### 4. ANALYSING THE SYSTEM PERFORMANCES

This section analyses the system performance both for ideal manipulators and robots with several dynamic phenomena at the joints namely, with nonlinear friction, backlash and flexibility. In order to compare the performance of the FDI algorithms we repeat the experiments with variable structure controllers (VSCs) [8-11]. The position and force controllers are the first-order VSCs with sliding surfaces and control efforts given by the equations ( $i = 1, 2$ ):

$$\mathbf{q}_{es} = \mathbf{J}_C^{-1} \mathbf{S} (\mathbf{Y}_{cd} - \mathbf{Y}_c) \quad (7a)$$

$$\sigma_i = \dot{q}_{esi} + c_{P_i} q_{esi} \quad (7b)$$

$$\tau_{VSC_i} = \begin{cases} \tau_{P_{max_i}} & , \sigma_i \geq \tau_{P_{max_i}} / K_{P_i} \\ K_{P_i} \sigma_i & , |\sigma_i| < \tau_{P_{max_i}} / K_{P_i} \\ -\tau_{P_{max_i}} & , \sigma_i \leq -\tau_{P_{max_i}} / K_{P_i} \end{cases} \quad (7c)$$

$$\tau_{est} = \mathbf{J}_C^T (\mathbf{I} - \mathbf{S}) (\mathbf{F}_d - \mathbf{F}) \quad (8a)$$

$$\sigma_i = \tau_{est} + c_{Fi} \int \tau_{est} dt \quad (8b)$$

$$\tau_{VSCi} = \begin{cases} \tau_{Fmaxi}, & \sigma_i \geq \tau_{Fmaxi} / K_{Fi} \\ K_{Fi} \sigma_i, & |\sigma_i| < \tau_{Fmaxi} / K_{Fi} \\ -\tau_{Fmaxi}, & \sigma_i \leq -\tau_{Fmaxi} / K_{Fi} \end{cases} \quad (8c)$$

Table III shows the numerical values of the VSCs adopted in this study [11] that were also tuned experimentally.

| Joint $i$ | $K_{Pi}$ | $K_{Fi}$ | $\tau_{Fmaxi}$ | $\tau_{Fmaxi}$ | $c_{Pi}$ | $c_{Fi}$ |
|-----------|----------|----------|----------------|----------------|----------|----------|
| 1         | $10^4$   | $10^2$   | $10^3$         | $10^3$         | 2.5      | 0.25     |
| 2         | $10^4$   | $10^2$   | 500            | 500            | 2.5      | 0.25     |

**Table III** Numerical values of the VSCs.

In the simulations, we study the system responses for  $\theta = \pi/2$  and the initial operating point  $q_{10} = q_{20} = 15\pi/36$ , where  $q_{i0}$  stands for the initial position of joint  $i$ . We apply a step at the force reference for  $t = 0$  (i.e.  $F_d = 1$  N) and a zero increment at the position input (i.e.  $y_{Cd} = y_{C0}$ ). The constraint surface parameters are  $M = 0.03$  Kg,  $B = 1$  Ns/m and  $K = 400$  N/m, being the sampling controller frequency  $f_c = 1$  kHz.

#### 4.1. IDEAL ROBOTS

In this subsection we compare the time response for the ideal 2R robot under the action of FDI and VSC algorithms (Figs. 3 and 4). As we can see the FDI scheme leads to a superior performance, namely to a smaller steady-state error and a faster transient.

#### 4.2. ROBOTS WITH NONLINEAR FRICTION

In this subsection we study the time response for the 2R robot with nonlinear friction at the joints.

Fig. 5 shows the model of the friction [15] employed in the robot joints where  $K$  is the Coulomb friction,  $B$  is the viscous

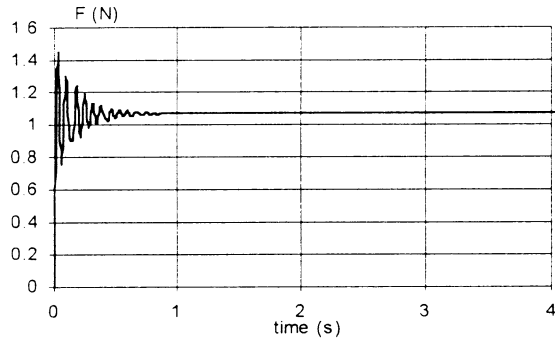


**Figure 3** Time response for the ideal 2R robot with the FDI algorithm (with  $\alpha_F = -1/5$ ).

friction and  $DV$  and  $F_H$  are the static friction parameters. In the simulations were adopted the values ( $i = 1, 2$ )  $K_i = 5$  Nm,  $B_i = 0.5$  Nms/rad,  $DV_i = 0.0025$  rad/s and  $F_{Hi} = 6$  Nm.

Comparing the FDI and the VSC responses (Figs. 6 and 7) we observe, once more, the superior performance of the fractional-order algorithm.

#### 4.3. ROBOTS WITH DYNAMIC BACKLASH

In this subsection we analyse the response of a 2R robot with dynamic backlash at the joints.

For the joint backlash (i.e. for a gear with clearance  $h_i$  at joint  $i$ ), we have impact phenomena between the inertias which obey the principle of conservation of momentum and the Newton's law, resulting:

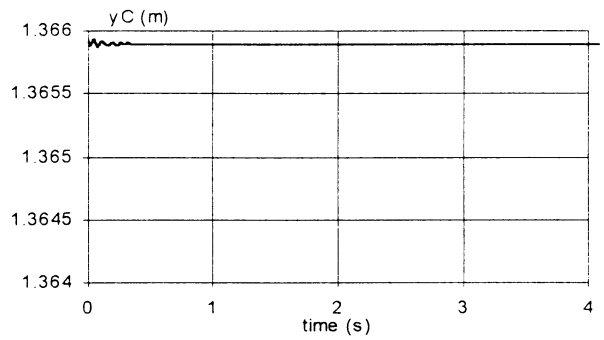
$$\dot{q}'_i = \frac{\dot{q}_i (J_{ii} - \varepsilon J_{im}) + \dot{q}'_{im} J_{im} (1 + \varepsilon)}{J_{ii} + J_{im}} \quad (9a)$$

$$\dot{q}'_{im} = \frac{\dot{q}_i J_{ii} (1 + \varepsilon) + \dot{q}'_{im} (J_{im} - \varepsilon J_{ii})}{J_{ii} + J_{im}} \quad (9b)$$

where  $0 < \varepsilon < 1$  is a constant that defines the type of impact ( $\varepsilon = 0$  inelastic impact,  $\varepsilon = 1$  elastic impact) and  $\dot{q}'_i$  and  $\dot{q}'_{im}$  are the velocities of the inertias of the joint and motor after the collision, respectively. The parameter  $J_{ii}$  ( $J_{im}$ ) stands for the link (motor) inertias of joint  $i$ . The numerical values adopted for the parameters were ( $i = 1, 2$ )  $h_i = 0.00018$  rad and  $\varepsilon_i = 0.5$ .

| Joint $i$ | $K_{Pi}$ | $K_{Fi}$ | $\alpha_{Pi}$ | $\alpha_{Fi}$ | $r_{Pi}$ | $r_{Fi}$ |
|-----------|----------|----------|---------------|---------------|----------|----------|
| 1         | 5000     | 50       | 1/2           | 1/5           | 17       | 17       |
| 2         | 5000     | 50       | 1/2           | 1/5           | 17       | 17       |

**Table IV** Numerical values of the FDI controllers re-tuned for backlash compensation.



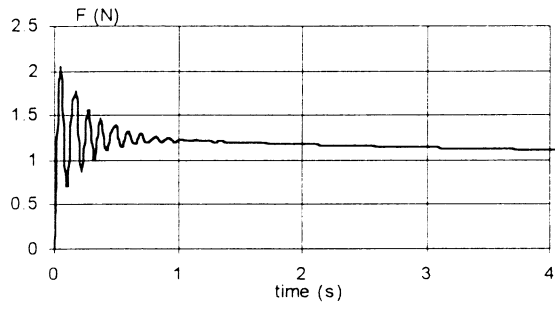


Figure 4 Time response for the ideal 2R robot with the VSC scheme.

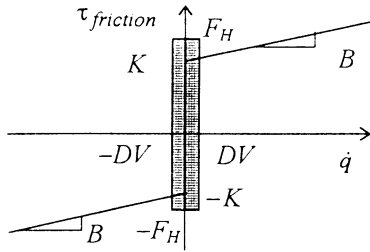
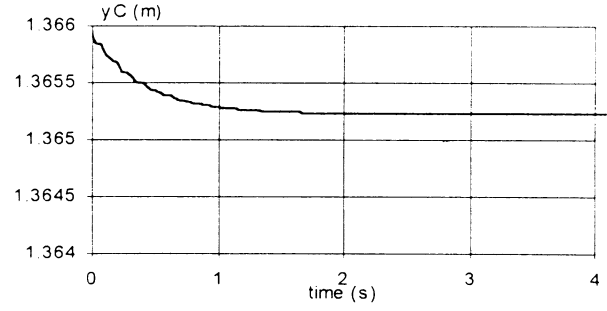


Figure 5 Model of the joint friction.

Fig. 8 shows the system response for the FDI scheme (with the parameters of Table II). Due to the unstable responses the algorithm was re-tuned with a fractional derivative action in the force loop (see Table IV). The responses with the new FDI

(Fig. 9) are somewhat superior to those of the VSC scheme (Fig. 10). Re-tuning the VSCs with  $(i = 1, 2) K_{P_i} = 5000$  and  $K_{F_i} = 500$ , we obtain a response similar to Fig. 9, but with a smaller force and a larger position steady-state errors.

#### 4.4. ROBOTS WITH FLEXIBLE JOINTS

For the case of the 2R robot with compliant joints, the dynamic model corresponds to (1) augmented by the equations:

$$\tau = \mathbf{J}_m \ddot{\mathbf{q}}_m + \mathbf{B}_m \dot{\mathbf{q}}_m + \mathbf{K}_m (\mathbf{q}_m - \mathbf{q}) \quad (10a)$$

$$\mathbf{K}_m (\mathbf{q}_m - \mathbf{q}) = \mathbf{H}(\mathbf{q}) \ddot{\mathbf{q}} + \mathbf{c}(\mathbf{q}, \dot{\mathbf{q}}) + \mathbf{g}(\mathbf{q}) - \mathbf{J}^T(\mathbf{q}) \mathbf{F} \quad (10b)$$

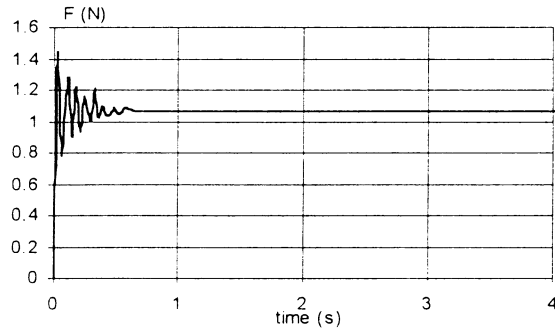


Figure 6 Time response for the 2R robot with nonlinear friction and the FDI algorithm (with  $\alpha_F = -1/5$ ).

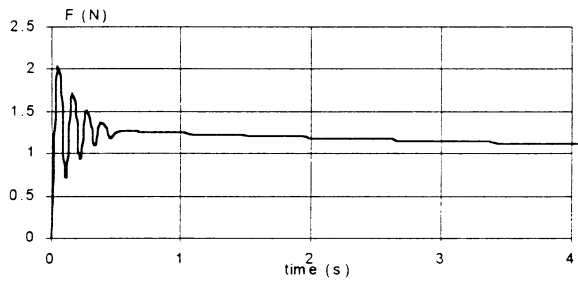
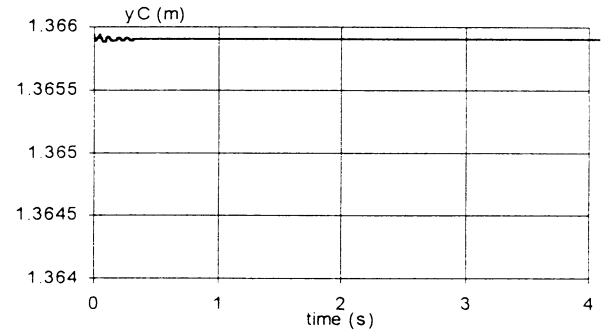
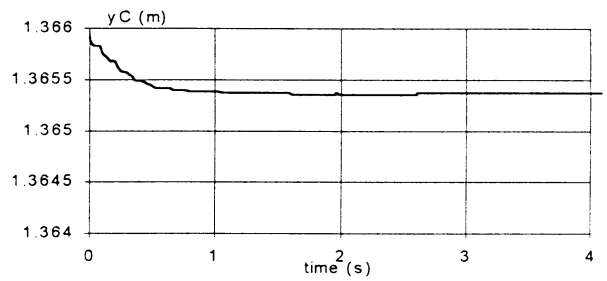
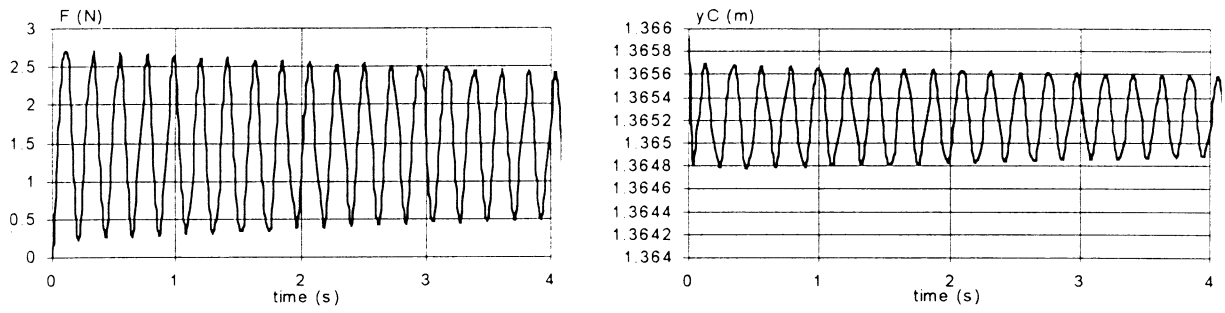
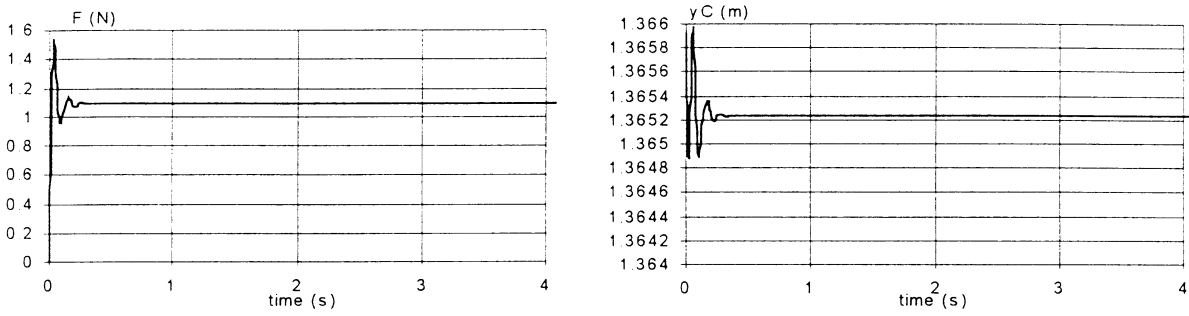


Figure 7 Time response for the 2R robot with nonlinear friction and the VSC scheme.





**Figure 8** Time response for the 2R robot with dynamic backlash and the FDI algorithm (with  $\alpha_F = -1/5$ ).



**Figure 9** Time response for the 2R robot with dynamic backlash and the re-tuned FDI algorithm (with  $\alpha_F = 1/5$ ).

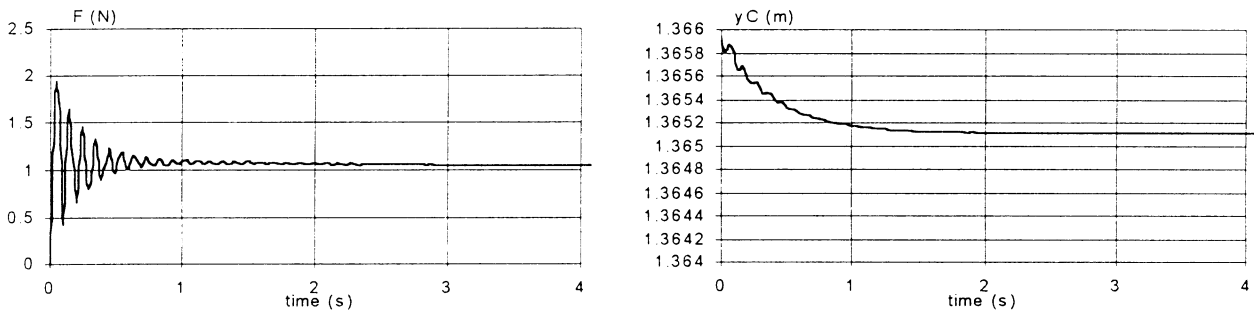


**Figure 10** Time response for the 2R robot with dynamic backlash and the VSC scheme.

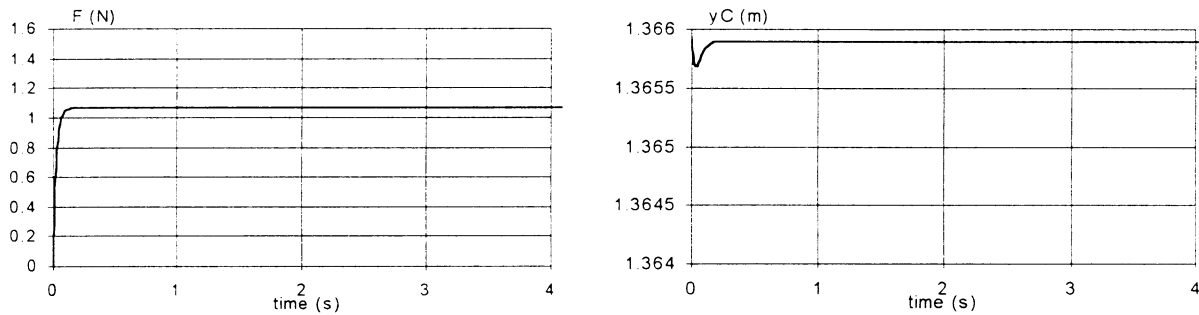


**Figure 11** Time response for the 2R robot with flexible joints and the FDI algorithm (with  $\alpha_F = -1/5$ ).

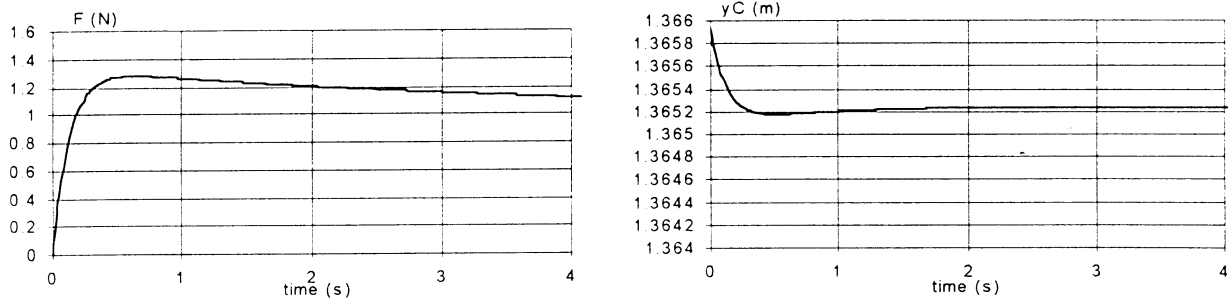


Figure 12 Time response for the 2R robot with flexible joints and the VSC scheme.

where  $\mathbf{J}_m$ ,  $\mathbf{B}_m$  and  $\mathbf{K}_m$  are the  $n \times n$  diagonal matrices of the motor and transmission inertias, damping and stiffness, respectively. In this case, for the simulations, it was adopted ( $i = 1, 2$ )  $K_{mi} = 2 \times 10^7$  Nm/rad and  $B_{mi} = 10^4$  Nms/rad. Analysing the responses we conclude that the FDI algorithm (Fig. 11) is, again, superior to the VSC scheme (Fig. 12).

## 5. CONCLUSIONS

This paper presented the implementation of hybrid fractional-order controllers for manipulators with several types of nonlinear phenomena at the joints. The system was tested both for FDI and VSC algorithms. The results showed that the FDI algorithms have superior performances, while the backlash problem seems to be the most difficult to deal with.

## ACKNOWLEDGEMENT

This paper was developed under the grant PRAXIS XXI/BD/4524/94 from FCT.

## 6. REFERENCES

- [1] M. H. Raibert and J. J. Craig, "Hybrid Position/Force Control of Manipulators", *ASME J. of Dyn. Syst., Meas., Control*, vol. 102, No. 2, pp. 126-133, 1981.
- [2] O. Khatib, "A Unified Approach for Motion and Force Control of Robot Manipulators: The Operational Space Formulation", *IEEE J. of Robotics and Automation*, vol. 3, No. 1, pp. 43-53, 1987.
- [3] W. D. Fisher and M. S. Mujtaba, "Sufficient Stability Condition for Hybrid Position/Force Control", *Proc. of the IEEE Int. Conf. on Robotics and Automation*, Nice, France, pp. 1336-1341, 1992.
- [4] H. Bruyninckx and J. De Schutter, "Specification of Force-Controlled Actions in the 'Task Frame Formalism' - A Synthesis", *IEEE Trans. on Robotics and Automation*, vol. 12, No. 4, pp. 581-589, 1996.
- [5] M. M. Bridges, J. Cai, D. M. Dawson and M. T. Grapple, "Experimental Results for a Robust Position and Force Controller Implemented on a Direct Drive Robot", *Robotica*, vol. 13, No. 1, pp. 11-18, 1995.
- [6] B. Siciliano and L. Villani, "A Force/Position Regulator for Robot Manipulators Without Velocity Measurements", *IEEE Int. Conf. on Robotics and Automation*, Minneapolis, USA, pp. 2567-2572, 1996.
- [7] R. Volpe and P. Khosla, "Computational Considerations in the Implementation of Force Control Strategies", *J. of Intelligent and Robotic Systems*, vol. 9, pp. 121-148, 1994.
- [8] A. Azenha and J. A. T. Machado, "Variable Structure Control of Robots with Nonlinear Friction and Backlash at the Joints", *1996 IEEE Int. Conf. on Robotics and Automation*, Minneapolis, USA, pp. 366-371, 1996.
- [9] V. I. Utkin, "Variable Structure Systems with Sliding Modes", *IEEE Trans. on Automatic Control*, vol. 22, pp. 212-222, 1977.
- [10] K.-K. D. Young, "Controller Design for a Manipulator Using Theory of Variable Structure Systems", *IEEE Trans. on Systems, Man, and Cybernetics*, vol. 8, No. 2, pp. 101-109, 1978.
- [11] A. Azenha and J. A. T. Machado, "Dynamic Analysis in Variable Structure Position/Force Hybrid Control of Manipulator", *Proc. of the IEEE Int. Conf. on Systems, Man, and Cybernetics*, Orlando, Florida, USA, pp. 4309-4314, 1997.
- [12] S. G. Samko, A. A. Kilbas and O. I. Marichev, "Fractional Integrals and Derivatives: Theory and Applications", Gordon and Breach Science Pub., 1993.
- [13] K. B. Oldham and J. Spanier, "The Fractional Calculus: Theory and Application of Differentiation and Integration to Arbitrary Order", Academic Press, 1974.
- [14] J. A. T. Machado, "Analysis and Design of Fractional-Order Digital Control Systems", *Journal of Systems Analysis, Modelling, and Simulation*, vol. 27, pp. 107-122, 1997.
- [15] B. Armstrong-Hélouvy, P. Dupont and C. C. de Wit, "A Survey of Models, Analysis Tools and Compensation Methods for the Control of Machines with Friction", *Automatica*, vol. 30, No. 7, pp. 1083-1138, 1994.